

Wireless power transfer to a cardiac implant

Sanghoek Kim, John S. Ho, Lisa Y. Chen, and Ada S. Y. Poon

Citation: *Appl. Phys. Lett.* **101**, 073701 (2012); doi: 10.1063/1.4745600

View online: <http://dx.doi.org/10.1063/1.4745600>

View Table of Contents: <http://apl.aip.org/resource/1/APPLAB/v101/i7>

Published by the [American Institute of Physics](#).

Related Articles

Microfluidic impedance spectroscopy as a tool for quantitative biology and biotechnology
Biomicrofluidics **6**, 034103 (2012)

Treatment of enterococcus faecalis bacteria by a helium atmospheric cold plasma brush with oxygen addition
J. Appl. Phys. **112**, 013304 (2012)

Biosensors for immune cell analysis—A perspective
Biomicrofluidics **6**, 021301 (2012)

The theory of modulated hormone therapy for the treatment of breast cancer in pre- and post-menopausal women
AIP Advances **2**, 011206 (2012)

Selective killing of ovarian cancer cells through induction of apoptosis by nonequilibrium atmospheric pressure plasma
Appl. Phys. Lett. **100**, 113702 (2012)

Additional information on *Appl. Phys. Lett.*

Journal Homepage: <http://apl.aip.org/>

Journal Information: http://apl.aip.org/about/about_the_journal

Top downloads: http://apl.aip.org/features/most_downloaded

Information for Authors: <http://apl.aip.org/authors>

ADVERTISEMENT

AEROTECH
nano Motion Technology

Click here for the **FREE**
nano Motion Technology Catalog

Linear Single-Axis and Dual-Axis Stages

Rotary Stages

Goniometers

Vertical Lift and Z Stages

The advertisement displays a variety of precision motion control components from Aerotech, including linear stages, rotary stages, goniometers, and vertical lift systems. A catalog is shown on the right side of the advertisement, listing features such as Long Travel, High Dynamic Performance, High Accuracy, High Resolution, and Aero-Drive Software.

Wireless power transfer to a cardiac implant

Sanghoek Kim, John S. Ho, Lisa Y. Chen, and Ada S. Y. Poon^{a)}
Stanford University, California 94305, USA

(Received 2 May 2012; accepted 30 July 2012; published online 13 August 2012)

We analyze wireless power transfer between a source and a weakly coupled implant on the heart. Numerical studies show that mid-field wireless powering achieves much higher power transfer efficiency than traditional inductively coupled systems. With proper system design, power sufficient to operate typical cardiac implants can be received by millimeter-sized coils. © 2012 American Institute of Physics. [<http://dx.doi.org/10.1063/1.4745600>]

Wireless power transfer to medical implants is desirable for removal of bulky energy storage components. Traditional analyses of wireless powering across human tissue operate in the near-field where the source and receiver consist of inductively coupled coils.^{1–3} Recently proposed systems for mid-range power transfer over air also occur in the near-field; high efficiency was obtained by tuning identical resonators to operate in the strongly coupled regime.^{4–6} Power transfer to medical implants, however, operates in the weakly coupled regime due to the asymmetry between the large external source and the small receiver on the implant. In this configuration, it was shown that the optimal power transfer occurs in the mid-field where energy is exchanged through a combination of inductive and radiative modes.⁷

Wireless powering is accomplished with the configuration shown in Figs. 1(a)–1(c). The external source consists of a resonator represented by a planar current density \mathbf{J}_1 that generates equivalent magnetic and electric fields. This formalism allows the source to be studied without assumptions on its underlying structure. The receiver is modeled as a small coil resonating at the same frequency as the source. The coil generates a magnetic dipole moment at an angle θ with respect to the normal to the source plane. Power transfer occurs through the time-varying magnetic field component in the direction of the dipole moment.

Previous analyses have obtained the optimal source current density for a multilayer tissue model.⁸ From the resulting fields in tissue \mathbf{H}_1 and \mathbf{E}_1 , the maximum power transfer efficiency was found. The performance of the system in an electromagnetic model of the human body, however, is also of interest. In this paper, we consider wireless power transfer across the human chest to an implant on the surface of the heart, as shown in Fig. 1(b). We show that in the mid-field, power sufficient to operate a typical implant can be delivered at a distance of 5 cm to millimeter-sized coils under tissue heating constraints.

Coupled-mode theory has been used to describe near-field wireless power transfer.^{4,5} The formalism, however, can be easily generalized to the mid-field. We obtain the following set of equations⁹:

$$\dot{a}_1(t) = (i\omega_1 - \Gamma_1)a_1(t) + \kappa a_2(t) + F_1 \quad (1)$$

$$\dot{a}_2(t) = (i\omega_2 - \Gamma_2 - \Gamma_L)a_2(t) + \kappa a_1(t), \quad (2)$$

where a_1 and a_2 are the mode amplitudes at the source and receiver respectively. κ is the coupling coefficient, F_1 the driving term, Γ_1 and Γ_2 the decay rates due to losses, and Γ_L the work extraction rate due to the load on the implant. The amplitudes are defined such that $|a_1|^2$ and $|a_2|^2$ correspond to the energy contained in the object. In the mid-field, κ is complex rather than purely imaginary such that a phase difference can exist between the source and receiver.

The source and receiver are in resonance when $\omega := \omega_1 = \omega_2$. At the steady-state, the mode amplitudes have a time dependency of $e^{i\omega t}$ and the power transfer efficiency is given by

$$\begin{aligned} \eta &= \frac{\Gamma_L |a_2|^2}{\Gamma_1 |a_1|^2 + (\Gamma_2 + \Gamma_L) |a_2|^2 + 2\text{Re}(\kappa)\text{Re}(a_1^* a_2)} \\ &= \frac{\frac{|\kappa|^2 \Gamma_L}{\Gamma_1 \Gamma_2 \Gamma_2}}{\left(1 + \frac{\Gamma_L}{\Gamma_2}\right) \frac{|\kappa|^2 + 2\text{Re}(\kappa)^2}{\Gamma_1 \Gamma_2} + \left(1 + \frac{\Gamma_L}{\Gamma_2}\right)^2}. \end{aligned} \quad (3)$$

The efficiency η is dependent on the matching ratio Γ_L/Γ_2 and is maximized when

$$\frac{\Gamma_L}{\Gamma_2} = \sqrt{1 + \frac{|\kappa|^2}{\Gamma_1 \Gamma_2} + \frac{2\text{Re}(\kappa)^2}{\Gamma_1 \Gamma_2}}. \quad (4)$$

In the weakly coupled regime, we have $|\kappa|^2 \ll \Gamma_1 \Gamma_2$. The efficiency in Eq. (3) can be approximated as

$$\eta \approx \frac{|\kappa|^2}{\Gamma_1 \Gamma_2} \frac{\Gamma_L/\Gamma_2}{(1 + \Gamma_L/\Gamma_2)^2} \quad (5)$$

which is the product of two factors: the coupling factor on the left and the matching factor on the right. The coupling factor is proportional to the ratio of the power available at the receiver to the input power. Similarly, the matching factor is related to the ratio of the power delivered to load to the available power.

Using standard power arguments, the matching ratio can be expressed as $\Gamma_L/\Gamma_2 = R_L/R_2$, where R_L is the load resistance and R_2 the real part of the self-impedance of the receive coil. When the source and receiver are weakly coupled, Eq. (4) states that the matching factor is maximized when $R_L \approx R_2$. Since R_2 is a parameter intrinsic to the coil and the

^{a)}Electronic mail: adapoon@stanford.edu.

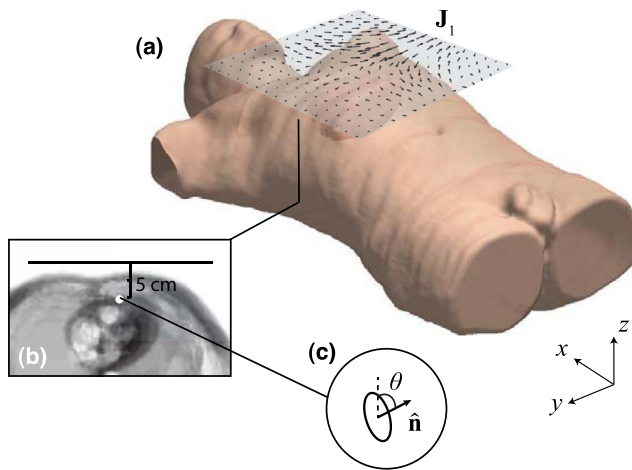


FIG. 1. Body model for wireless power transfer to a cardiac implant. (a) Source plane modeled by current density \mathbf{J}_1 . (b) Source position 5 cm above a small receive coil (white dot) on the heart. (c) Receive coil orientation at angle θ .

surrounding tissue, impedance matching is usually achieved by the appropriate choice of R_L . The ideal matching condition, however, cannot always be satisfied since very small values of R_L are infeasible for most implants.¹⁰

The coupling factor can also be related to the physical fields by power arguments. In particular, we find that $|\kappa|^2/(\Gamma_1\Gamma_2) = |V_{oc}|^2/(2R_2P_1)$. V_{oc} is the open-circuit voltage induced at the receiver due to the coupling κ between the source and receiver. R_2 , the real part of the receiver self-impedance due to Γ_2 , is dependent on the surrounding tissue. P_1 is the power loss due to Γ_1 and is usually dominated by tissue loss. For a receive coil at \mathbf{r}_f with area A_r and direction $\hat{\mathbf{n}}$, we define a parameter

$$k = \frac{|V_{oc}|^2}{2P_1} = \frac{\omega\mu_0^2 A_r^2 |\mathbf{H}_1(\mathbf{r}_f) \cdot \hat{\mathbf{n}}|^2}{\int \text{Im } \epsilon(\mathbf{r}) |\mathbf{E}_1(\mathbf{r})|^2 d\mathbf{r}} \quad (6)$$

which is determined only by the source fields. It can be seen from Eq. (6) that as ω increases, the induced voltage V_{oc} also increases. However, this increase in k can be offset by dielectric losses, which also increase with frequency, suggesting that an optimal frequency exists.

The optimal η is determined from Eq. (5) by the following procedure. First, the source current density \mathbf{J}_1 generating fields \mathbf{H}_1 and \mathbf{E}_1 that maximize k is found. Next, R_2 for the receive coil is evaluated; the coupling factor is given by k/R_2 . Finally, the matching factor is determined by setting R_L as close to R_2 as possible, taking into consideration a minimum feasible R_L . In the following studies, we seek to determine the frequency f , receiver orientation θ , and receiver radius r that enable efficient power transfer.

We compute the fields with the finite-difference-time-domain (FDTD) method over a computational model of the body.¹¹ Dielectric dispersion is modeled by Debye relaxation; the parameters for this model have been extensively tabulated for human tissue.¹² The source \mathbf{J}_1 is simulated as a 15×15 grid of electric dipoles equally spaced 8 mm apart with arbitrary orientation on the plane. These dimensions were found sufficient to closely approximate the optimal current sheet for the multilayer model.⁸ The weights maximiz-

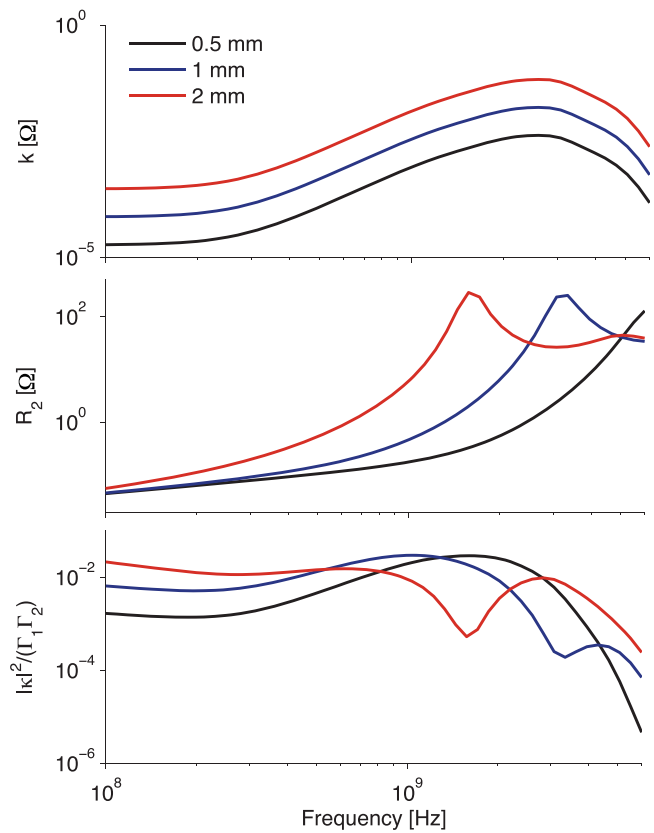


FIG. 2. Theoretical k , receiver self-resistance R_2 , and coupling factor $|\kappa|^2/(\Gamma_1\Gamma_2)$ as a function of frequency for a receive coil of radius 0.5, 1, and 2 mm. Results are obtained on the multilayer model.

ing k are numerically found by separately evaluating the fields for the x and y components of each dipole. From the resulting fields in tissue, the optimal weights can be obtained through a matrix inversion.¹³ The receiver R_2 is analytically obtained for a coil surrounded by heart tissue. The minimum R_L is set to 10 Ω , corresponding to a typical load of 1 k Ω and a maximum impedance transformation ratio of 1:100, since quality factors of at most 10 are feasible on implants.¹⁴ In addition to FDTD calculation, we obtain a theoretical η using the multilayer tissue model, for which the field and optimal source current density have an analytical expression.

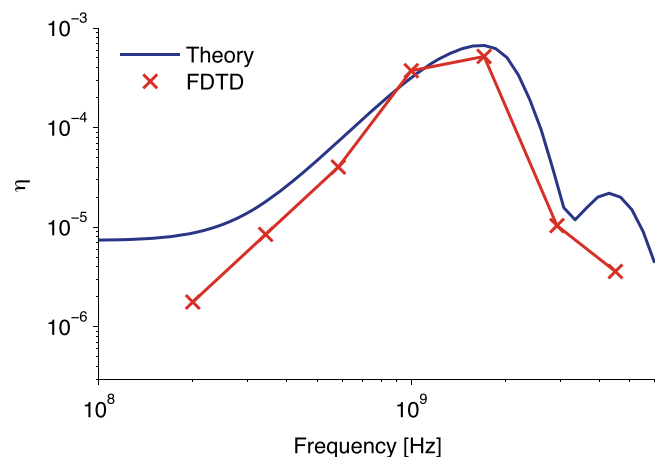


FIG. 3. Efficiency η as a function of frequency. The receiver is a 1-mm radius coil oriented $\theta = 90^\circ$ on the heart. Theory results are obtained on the multilayer model and the FDTD results on the body model.

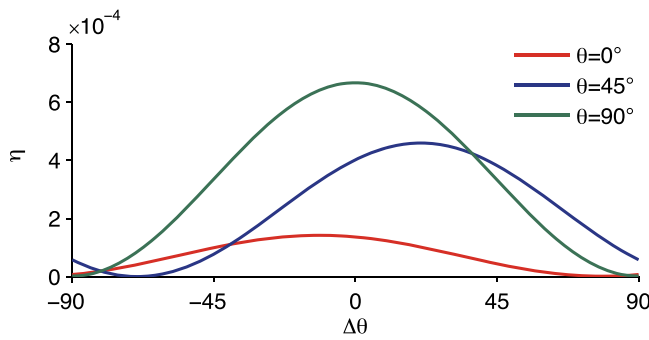


FIG. 4. Efficiency as a function of coil angular displacement at 1.7 GHz for sources optimized for the $\theta = 0^\circ$, 45° , and 90° receive coil orientations.

The tissue layers and thicknesses for the model are chosen to approximate the chest wall.

Fig. 2 shows the theoretical k , R_2 , and $|\kappa|^2/(\Gamma_1\Gamma_2)$ as a function of frequency for receive coils of radii 0.5, 1, and 2 mm. Since $|\kappa|^2/(\Gamma_1\Gamma_2) \ll 1$, the system is in the weakly coupled regime. R_2 exhibits a peak due to self-resonance when the wavelength in tissue coincides with the coil diameter. The resulting efficiency for the 1-mm coil is shown in Fig. 3. For the body model, the maximum efficiency $\eta = 4.45 \times 10^{-4}$ occurs at about 1.7 GHz and is more than an order of magnitude greater than efficiencies in the MHz range. For wavelengths in tissue, 1.7 GHz corresponds to operation in the mid-field. The FDTD results closely matches the theoretical calculations around 1 GHz. However, below 300 MHz or above 3 GHz, the results deviate since the FDTD source and body model are no longer well approximated by the multilayer model. Since the results are in agreement at the frequencies of interest, we will consider only the body model for the rest of this paper.

We next examine the effect of coil orientation on efficiency. We obtain the optimal source for a receiver oriented at $\theta = 0^\circ$, 45° , and 90° and consider the magnetic field at the receiver. Fig. 4 shows the efficiency when the receive coil tilted in the θ direction such that the source and receiver are mismatched. With no angular displacement, $\theta = 90^\circ$ has the highest efficiency even for large mismatch angles. For the $\theta = 45^\circ$ configuration, the efficiency actually increases

slightly when the coil is rotated towards the transverse plane. This effect is due to the fact that the transverse component of the magnetic field is dominant at the receiver, which is characteristic of electromagnetic fields beyond the near-field. Unlike the far-field, however, the magnetic field component in the direction of propagation is significant, as shown by the efficiency obtained at $\theta = 0^\circ$. This confirms that the system is operating in the mid-field. The optimal orientation in this case is $\theta = 90^\circ$ rather than $\theta = 0^\circ$ as in the near-field.⁵

In order to determine the power transferred to the receiver from the efficiency, we consider the maximum transmit power. At the frequencies of interest, the transmit power is limited by tissue heating. This is often measured by the specific absorption rate (SAR) and should not exceed 1.6 mW/cm^3 according to the IEEE safety guidelines.¹⁵ As an useful reference, we normalize the transmit power such that the maximum SAR is equal to the safety limit. Fig. 5 shows the resulting open-circuit voltage V_{oc} available at each point in the body at 200 MHz and 1.7 GHz. The corresponding SAR distribution in the body is also shown in Fig. 5. For the same maximum heating, the available voltage is much greater at the low-GHz range; the $|V_{oc}|^2$ is $8.7 \times 10^{-4} \text{ V}^2$ at 1.7 GHz and drops to $1.1 \times 10^{-5} \text{ V}^2$ at 200 MHz. In the mid-field, the power is “focused”; that is, the fields interfere constructively at the receiver but destructively otherwise to minimize tissue heating. This effect is not observed at 200 MHz since interference effects are not significant at distances less than the wavelength.

Finally, we consider the relationship between the receive coil size and the transferred power. Fig. 6 shows the received open-circuit voltage V_{oc} and the received power versus the coil radius at 1 and 1.7 GHz. P_r drops at the R_2 resonant peak; however, for a given radius, this drop can be avoided by operating away from the peak. For a 1-mm radius coil, an open-circuit voltage of 47.7 mV and received power of $51.2 \mu\text{W}$ can be obtained. For typical quality factors, this voltage is sufficient for generating potentials exceeding the threshold voltage of typical transistors. The received power also meets the power consumption demands of many implants; a pacemaker consuming $8 \mu\text{W}$, for example, was reported by Wong *et al.*¹⁶ Such millimeter-sized coils are

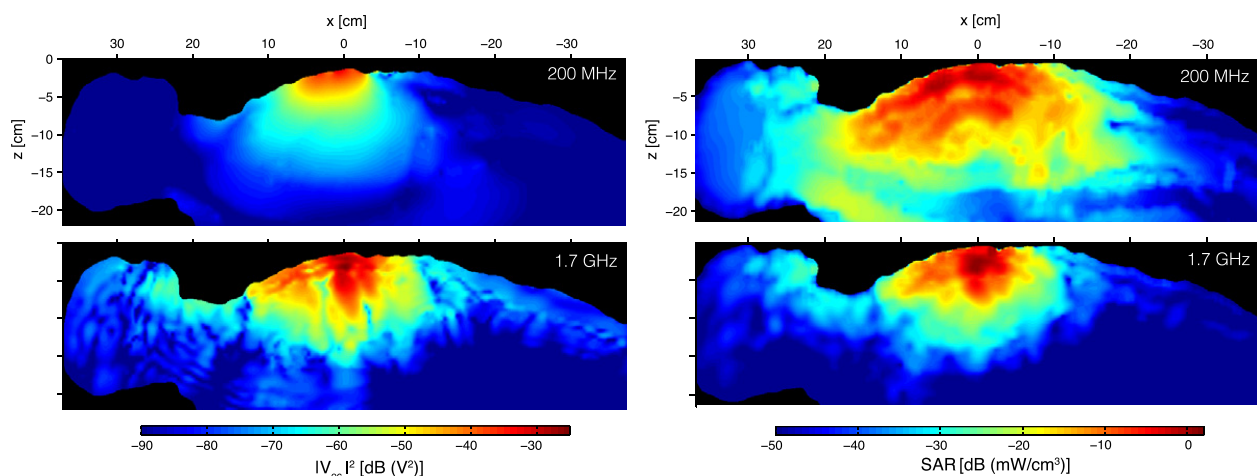


FIG. 5. Available open-circuit voltage $|V_{oc}|^2$ and SAR distribution along the $y=0$ slice of the model at 200 MHz and 1.7 GHz. The receiver is a 1-mm coil tilted $\theta = 90^\circ$ is placed at a depth of 5 cm.

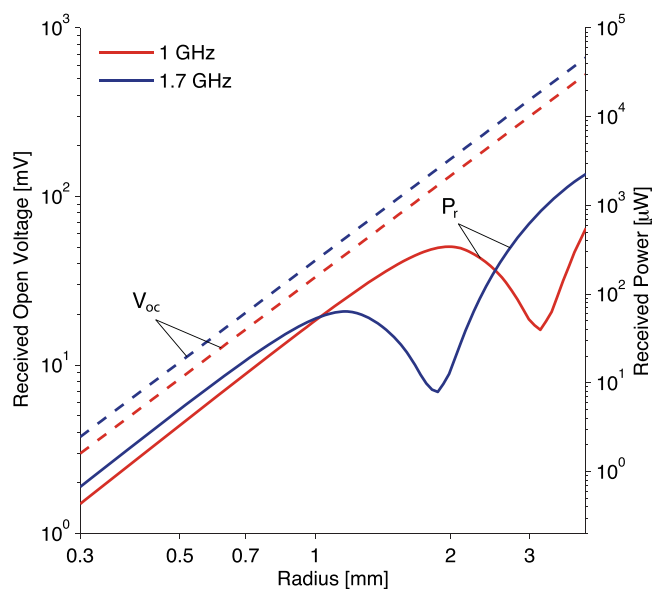


FIG. 6. Received open circuit V_{oc} and received power P_r as a function of the receive coil radius at 1 GHz and 1.7 GHz. The coil is oriented $\theta = 90^\circ$.

much smaller than receivers designed for near-field operation, which are typically several centimeters in size.^{17,18}

In conclusion, we study mid-field wireless powering between a weakly coupled source and receiver in an electromagnetic model of the human body. The optimal frequency and the orientation of a receive coil placed on the surface of the heart are consistent with operation in the mid-field. Under tissue heating constraints, power sufficient to operate a typical implant can be received by a 1-mm radius coil. We note that while our results were obtained for a source mod-

eled by an arbitrary current density, in practice, the current density must be synthesized by a physical antenna. The design of such an antenna remains to be addressed in future work.

- ¹F. C. Flack, E. D. James, and D. M. Schlapp, *Med. Biol. Eng.* **9**, 79–85 (1971).
- ²W. H. Ko, S. P. Liang, and C. D. F. Fung, *Med. Biol. Eng. Comput.* **15**, 634–640 (1977).
- ³W. J. Heetderks, *IEEE Trans. Biomed. Eng.* **35**, 323–327 (1988).
- ⁴A. Kurs, A. Karalis, R. Moffatt, J. D. Joannopoulos, P. Fisher, and M. Soljacic, *Science* **317**, 83–86 (2007).
- ⁵X. Yu, S. Sandhu, S. Beiker, R. Sassoon, and S. Fan, *Appl. Phys. Lett.* **99**, 214102 (2011).
- ⁶I. Sasada, *J. Appl. Phys.* **111**, 07E733 (2012).
- ⁷A. S. Y. Poon, S. O'Driscoll, and T. H. Meng, *IEEE Trans. Antennas Propag.* **58**, 1739–1750 (2010).
- ⁸S. Kim, J. S. Ho, and A. S. Y. Poon, "Wireless power transfer to miniature implants: transmitter optimization," *IEEE Trans. Antennas Propag.* (to be published).
- ⁹H. A. Haus, *Waves and Fields in Optoelectronics* (Prentice-Hall, Englewood Cliffs, NJ, 1984).
- ¹⁰E. Perret, S. Tedjini, and R. S. Nair, *Proc. IEEE* **100**, 2330–2340 (2012).
- ¹¹G. Zubal, C. R. Harrell, E. O. Smith, Z. Rattner, G. Gindi, and P. B. Hoffer, *Med. Phys.* **21**, 299–302 (1994).
- ¹²S. Gabriel, R. W. Lau, and C. Gabriel, *Phys. Med. Biol.* **41**, 2271–2293 (1996).
- ¹³S. Kim and A. S. Y. Poon, in *IEEE Antennas and Propagation Society International Symposium (APSURSI)*, Spokane, WA, 2010.
- ¹⁴T. H. Lee, *The Design of CMOS Radio-Frequency Integrated Circuits* (Cambridge University Press, Cambridge, U.K., 1998).
- ¹⁵"IEEE standard for safety with respect to human exposure to radio-frequency electromagnetic fields, 3 kHz to 300 GHz," *IEEE Standard C95.1-1991* (1999).
- ¹⁶L. S. Y. Wong, S. Hossain, A. Ta, J. Edvinsson, D. H. Rivas, and H. Naas, *IEEE J. Solid-State Circuits* **39**, 2446–2456 (2004).
- ¹⁷G. J. Suanning and N. H. Lovell, *IEEE Trans. Biomed. Eng.* **48**, 248–260 (2001).
- ¹⁸Y. M. Hu and M. Sawan, *IEEE Trans. Circuits Syst. I, Reg. Pap.* **52**, 2552–2562 (2005).